Published in final edited form as:
Clin Cancer Res. 2012 January 1; 18(1): 184–195. doi:10.1158/1078-0432.CCR-11-1558.

Antitumor Activity of NVP-BKM120–A Selective Pan Class I PI3 Kinase Inhibitor Showed Differential Forms of Cell Death Based on p53 Status of Glioma Cells

Dimpy Koul[1], **Jun Fu**[1], **Ruijun Shen**[1], **Tiffany A. LaFortune**[1], **Shuzhen Wang**[1], **Ningyi Tiao**[1], **Yong-Wan Kim**[1], **Juinn-Lin Liu**[1], **Deepti Ramnarian**[1], **Ying Yuan**[2], **Carlos Garcia-Echevrria**[3], **Sauveur-Michel Maira**[3], and **W.K. Alfred Yung**[1]

[1]Department of Neuro-Oncology, Brain Tumor Center, The University of Texas M. D. Anderson Cancer Center, Houston, Texas [2]Department of Biostatistics, The University of Texas M. D. Anderson Cancer Center, Houston, Texas [3]Novartis Institutes for Biomedical Research, Oncology Drug Discovery, Klybeckstrasse, Basel, Switzerland

Abstract

Purpose—The aim of this study was to show preclinical efficacy and clinical development potential of NVP-BKM120, a selective pan class I phosphatidylinositol-3 kinase (PI3K) inhibitor in human glioblastoma (GBM) cells *in vitro* and *in vivo*.

Experimental Design—The effect of NVP-BKM120 on cellular growth was assessed by CellTiter-Blue assay. Flow cytometric analyses were carried out to measure the cell-cycle, apoptosis, and mitotic index. Mitotic catastrophe was detected by immunofluorescence. The efficacy of NVP-BKM120 was tested using intracranial U87 glioma model.

Results—We tested the biologic effects of a selective PI3K inhibitor NVP-BKM120 in a set of glioma cell lines. NVP-BKM120 treatment for 72 hours resulted in a dose-dependent growth inhibition and effectively blocked the PI3K/Akt signaling cascade. Although we found no obvious relationship between the cell line's sensitivity to NVP-BKM120 and the phosphatase and tensin homolog (*PTEN*) and epidermal growth factor receptor (EGFR) statuses, we did observe a differential sensitivity pattern with respect to p53 status, with glioma cells containing wild-type p53 more sensitive than cells with mutated or deleted p53. NVP-BKM120 showed differential forms of cell death on the basis of p53 status of the cells with p53 wild-type cells undergoing apoptotic cell death and p53 mutant/deleted cells having a mitotic catastrophe cell death. NVP-BKM120 mediates mitotic catastrophe mainly through Aurora B kinase. Knockdown of p53 in p53 wild-type U87 glioma cells displayed microtubule misalignment, multiple centrosomes, and mitotic catastrophe cell death. Parallel to the assessment of the compound in *in vitro* settings, *in vivo* efficacy studies using an intracranial U87 tumor model showed an increased median survival from 26 days (control cohort) to 38 and 48 days (treated cohorts).

Corresponding Author: W.K. Alfred Yung, Department of Neuro-Oncology, Brain Tumor Center, Unit 431, The University of Texas M. D. Anderson Cancer Center, 1515 Holcombe Blvd., Houston, TX 77030. Phone: 713-794-1285; Fax: 713-794-4999; wyung@mdanderson.org.

Supplementary data for this article are available at Clinical Cancer Research Online (http://clincancerres.aacrjournals.org/).

Disclosure of Potential Conflicts of Interest W.K.A. Yung has a commercial research grant from Novartis and is a consultant/advisory board member for Merck, Eden, and Exelixis. No potential conflicts of interest were disclosed by the other authors.

Conclusion—Our present findings establish that NVP-BKM120 inhibits the PI3K signaling pathways, leading to different forms of cell death on the basis of p53 statuses. Further studies are warranted to determine if NVP-BKM120 has potential as a glioma treatment.

Introduction

The phosphatidylinositol-3 kinase (PI3K) pathway is a key signal transduction system that links oncogenes and multiple receptor classes to many essential cellular functions and is one of the most commonly activated signaling pathway in human cancer. This pathway therefore presents both an opportunity and a challenge for cancer therapy in solid tumors and hematologic malignancies (1). Ample genetic and laboratory studies suggest that the PI3K/Akt pathway is vital to the growth and survival of cancer cells. Because there are multiple possible causes of PI3K activation, there are also several possible therapeutic approaches that may be taken to target cancer cells by means of PI3K inhibition and the clinical benefit of the different therapies may vary that affects both the most effective therapeutic approach and the likelihood of clinical benefit from PI3K inhibition.

Several genetic abnormalities are known to activate PI3K/Akt signaling. The first genetic mechanism identified was loss of the phosphatase and tensin homolog (*PTEN*) tumor suppressor, which encodes a phosphatidylinositol-3, 4, 5-trisphosphate (PIP_3) 3′-phosphatase that turns off the PI3K pathway (2–5). Although loss of *PTEN* is tumorigenic, it is unclear if *PTEN* loss alone is sufficient to activate PI3K. Indeed, recent studies have shown that some receptor tyrosine kinase (RTK) inhibitors have therapeutic potential because they can down regulate Akt even when PTEN expression is lost (6). Although loss of *PTEN* might not absolutely preclude the capacity for RTK inhibitors to shut off PI3K signaling, it seems to reduce the likelihood of cancers responding to these therapies as single agents (7–10).

Somatic activating mutations were recently identified in the class I_A PI3K catalytic subunit, p110α [encoded by *PIK3CA* (11)]. Somatic mutations in *PIK3CA* occur in up to 30% of some types of common epithelial cancer, which includes breast, colon, prostate, and endometrial cancers (11) Recent data suggest that some cancers harbor activating mutations in the PI3K regulatory subunit, p85 (encoded by *PIK3R1*). The Cancer Genome Atlas Research Network identified *PIK3R1* mutations in 9 of 91 human glioblastomas (GBM; ref. 12). In addition, our own TCGA data analysis also identified *PTEN* mutation in 48 of 157 human GBMs (30.6%) with 74% samples showing *PTEN* loss and 9% showing *PTEN* deletion (Personal communication). The *PTEN* tumor suppressor is a central negative regulator of the PI3K/Akt signaling cascade that influences multiple cellular functions including cell growth, survival, proliferation, and migration in a context-dependent manner.

PI3K activation initiates a signal transduction cascade that promotes cancer cell growth, survival, and metabolism. Akt, a serine-threonine kinase that is directly activated in response to PI3K, is a major effector of PI3K in cancers. The PIP_3 generated by activation of the PI3Kα isoform or sustained by the inactivation of *PTEN* binds to a subset of lipid-binding domains in downstream targets, such as the pleckstrin homology domain of the oncogene Akt (13, 14), thereby recruiting it to the plasma membrane. Once at the plasma membrane, Akt can be fully activated (15, 16). The downstream effects of the PI3K inhibition are very complex and depend on the biochemical features and molecular background of the cell type. The reported cell-cycle effects are predominantly G_1 (17, 18) and G_2-M block (19, 20). The G_2-M arrest has been observed independently of p53 and Rb status, yet several key regulatory proteins of G_2-M transition (Chek1, Cdk1, Wee1, Myt1, and Polo-1 kinase) have been identified targets of PI3K which may explain the substantial G_2-M peak in cell cycle on treatment. Failure to arrest the cells at or before mitosis results in formation of

micronucleated cells, aberrant segregation of chromosomes, microtubule misalignment, multicentrosomes, multipolar mitoses, and aneuploidy, leading to eventual cell death (21). Mitotic catastrophe is a term used to describe these failures in mitosis, reported previously in literature (22–25). Accumulating evidence has implicated p53 as a key regulator of the DNA damage checkpoint response, the S and G_2-M checkpoint (26, 27). Studies by Jin and colleagues show that G_2-M checkpoint is complex and may involve redundant controls including both p53 independent and p53-dependent mechanisms.

Many of the PI3K inhibitors currently in pre- or clinical development inhibit all of the catalytic subunit isoforms of class I_A PI3Ks (p110α, p110β, and p110γ). However, it remains unclear which type of inhibitor would be more effective clinically, isoform-specific inhibitors or pan-PI3K inhibitors. Therefore, we tested the effect of NVP-BKM120—a pan class I PI3K inhibitor in glioma cells. We observed that PI3K activity blockade by NVP-BKM120 induces G_2-M cell-cycle arrest *in vitro*. Interestingly, this drug exerts its effects in a p53-dependent manner with p53 wild-type cells undergoing apoptosis and p53-mutant/deleted cells undergoing mitotic catastrophe through the regulation of Aurora B kinase protein. In addition, NVP-BKM120 treatment prolonged the median survival of mice with intracranial xenograft tumors without causing any obvious toxic effects; a finding supporting the use of NVP-BKM120 inhibition of the PI3K/Akt pathway as a safe and effective therapy for cancers with aberrant *PTEN*/and/or high PI3K expression.

Materials and Methods

Cell lines

Twenty-one glioma cell lines with various p53 and *PTEN* statuses were maintained as monolayer cultures in Dulbecco's Modified Eagle Medium (DMEM)/F12 supplemented with 10% FBS and penicillin-streptomycin (all from Life Technologies, Inc.).

Reagents

NVP-BKM120 (28) was provided by Novartis Pharma AG through a material transfer agreement with The University of Texas M. D. Anderson Cancer Center (Houston, TX). For *in vitro* use, NVP-BKM120 was dissolved in dimethyl sulfoxide (DMSO; Sigma-Aldrich) to a concentration of 10 mmol/L, stored at −20°C, and further diluted to an appropriate final concentration in DMEM at the time of use. DMSO in the final solution did not exceed 0.1% (v/v). For *in vivo* studies NVP-BKM120 was dissolved in 1 volume of NMP (1-methyl-2-pyrrolidone). After dissolution, 9 volumes of PEG300 were added. The final ratio was NMP 10%/PEG300 90%. Once in solution, animals were treated in the next 30 minutes to1 hour.

Growth inhibition assays

Cells were seeded in 96-well plates (5,600 cells per well) and incubated at 37°C for 24 hours before addition of serial dilutions of NVP-BKM120. Growth inhibition was determined using the CellTiter-Blue (Promega) viability assay. The IC_{50} value was calculated as the mean drug concentration required to inhibit cell proliferation by 50% compared with vehicle controls.

Cell-cycle and apoptosis analysis

Glioma cells were plated at a density of 3×10^5 cells per well in 60-mm plates and maintained in 10% FBS-containing medium overnight. The following day, the cells were washed twice and treated with NVP-BKM120 in 10% FBS-containing medium. Seventy-two hours later, cells were fixed in 70% ethanol in PBS and stored at −20° C for 24 hours. Propidium iodide staining of DNA was carried out to determine the distribution of cells at different phases of the cell cycle. Cells for DNA analysis were fixed in 1%

paraformaldehyde, stored in 70% ethanol, and analyzed for apoptosis by flow cytometry using the Annexin V Kit (Phoenix Flow Systems) according to the manufacturer's instructions. Samples were analyzed using a BD FACS Calibur Flow Cytometer and Cell Quest software (BD Biosciences).

We also investigated the effect of NVP-BKM120 on the expression of apoptotic proteins. In particular, we determined the effect of inhibitor treatment on PARP, a well-known substrate for caspase-3, 6, and 7, and caspase-3 to determine whether inhibitor-induced apoptosis was mediated through caspase activation. In this experiment, glioma cells were treated with NVP-BKM120 for 24, 48, and 72 hours, after which whole-cell extracts were prepared and analyzed for cleavage of PARP and caspase-3. Immunoblot analysis was then carried out to determine the activation status of the downstream caspases.

Western blot analysis

Subconfluent monolayers of cells were treated with NVP-BKM120 at various doses in serum-free medium. Four hours later, cells were harvested and then either stimulated with epidermal growth factor (EGF; 50 ng/mL) for 10 minutes or left untreated. The cells were harvested in lysis solution as previously described (29) and subjected to Western blot analysis. Membranes were probed with the following primary antibodies: phospho-specific Akt (Ser-473 and Thr-308), total Akt, phospho-S6K1, total S6K1, phospho-S6, total S6, and phospho-Aurora B kinase, Aurora B kinase, and p53 (all from Cell Signaling). Anti-β-actin antibody was purchased from Sigma.

Indirect immunofluorescence

Immunofluorescence staining was carried out as described previously (30). Briefly, cells were seeded at a concentration of 2×10^5 cells per well in 6-well plates with coverslips inside and left overnight. The following day, the cells were treated with the indicated dose of NVP-BKM120 for 72 hours, media were aspirated, and the cells were washed with PBS once before being fixed with 3.7% formaldehyde in PBS for 20 minutes. After another PBS wash, the cells were permeabilized with 0.1% Triton X-100 in PBS for 5 minutes and then blocked with 3% bovine serum albumin-0.1% Tween 20-PBS for 1 hour. Cells were then incubated with mouse primary antibodies against F-actin for 1 hour. After 2 washes with PBS (containing 0.1% Tween 20), the cells were incubated with Alexa Fluor 488 anti-mouse secondary antibody (Molecular Probes) and was applied subsequently. Nuclear morphology was visible with 4',6-diaminidino-2-phenylindole (Molecular Probes). Images were processed with the Olympus software (Olympus).

Mitotic index

Cells were treated with 2 μm of NVP-BKM120 or DMSO (0.1%) for 72 hours and stained according to the manufacturer's instructions with phospho-histone H3 (Ser^{10}) antibody, Alexa Fluor 488-conjugated antibody (Cell Signaling Technology) and PI. In this assay, the fraction of cells that incorporates PI and co stains with anti-phospho-his-tone H3 antibody is considered as to be at the onset of mitosis. The percentage of mitotic cells was determined by fluorescence-activated cell-sorting analysis.

Specific knockdown of p53 by lentiviral short hairpin RNA

U87 cells were infected with the p53 short hairpin RNA (shRNA; Santa Cruz Biotechnology Inc.). Twenty-four hours later, cells were treated with NVP-BKM120 for another 72 hours. Cells were harvested after 5 days either for Western blot analysis or fixed for staining with phosphohistone H3 and F-actin as described above.

Animal studies

All animal studies were conducted in the veterinary facilities of M. D. Anderson Cancer Center in accordance with institutional rules, state and federal laws, and ethical guidelines for experimental animal care. We examined the antitumor efficacy of NVP-BKM120 in intracranial xeno-grafts derived from U87 cells. Nude (*nu*/*nu*) 6- to 8-week-old mice (10 animals in each group) were obtained from the M. D. Anderson breeding facility. To create the intracranial disease model, we engrafted U87 human GBM cells (5×10^5) into the caudate nucleus of each mouse using a previously described guide-screw system (31) and then randomly divided the mice into 4 groups of 10 mice each. Starting on day 4 after the tumor cells were implanted, mice were treated by oral gavage with 20 or 40 mg/kg once per day with NVP-BKM120 in NMP/PEG300 or NMP/PEG300 alone (control) on a 5-days-on, 2-days-off schedule for 4 weeks. At 2 and 4 weeks, 2 animals from each group were euthanized for biologic assessment of tumor response or tolerability with respect to body weight, water intake, and general activity. At necropsy, all organs were analyzed grossly and microscopically to assess tolerability at the tested doses.

Immunohistochemical staining

Sections (5-μm thick) of formalin-fixed, paraffin-embedded whole brains from control vehicle and NVP-BKM120- treated animal specimens were stained with anti p-Akt, cleaved PARP, cleaved caspase-3 (all from Cell Signaling), and Ki-67 (BD Biosciences). The sections were visualized by using a diaminobenzidine substrate kit. The slides were examined under a bright-field microscope.

Results

Pharmacokinetics of NVP-BKM120

NVP-BKM120 (Fig. 1A) inhibits PI3K activity by binding to the ATP binding cleft of this enzymes and was tested against class I PI3K and other kinases using an ATP depletion (Kinase-Glo) assay (Table 1). The compound was shown to be active against P110 α, β, and γ. Further characterization of NVP-BKM120 has shown that it poorly inhibits a representative panel of protein kinases in biochemical assays (Table 1).

NVP-BKM120 inhibited cell growth of glioma cells

We tested NVP-BKM120 against a panel of 21 glioma cell lines that differed in terms of the mutational statuses of *PTEN* and *p*53. NVP-BKM120 potently inhibited glioma cell proliferation in all the lines, with IC_{50} values in the cell viability assay of 1 to 2 μmol/L (Fig. 1B). Although no obvious relationship existed between sensitivity to NVP-BKM120 and *PTEN* status, we did observe a differential sensitivity pattern with respect to p53 status, with wild-type p53 cells being more sensitive to NVP-BKM120 than p53-mutant/deleted glioma cells (Fig. 1C, *P*-value < 0.0001). The p53 and *PTEN* statuses of the glioma cells are shown in Fig. 1C. The relative sensitivity of the glioma cancer cell lines to NVP-BKM120 was calculated relative to the mean IC_{50} of LN751 cells using the equation: $-\log_2$ (IC_{50} individual cell line/IC_{50} of LN751). The p53 wild-type cell lines had a significantly lower average IC_{50} than p53-mutant/deleted cell lines (*P*-value < 0.0001). The average IC_{50} for the p53 wild-type cell lines was 1.28 with a SD of 0.33, whereas that for the p53-mutant/deleted cell lines was 2.08 with a SD of 0.69. (Fig. 1D). In contrast, the *PTEN* status did not have a significantly effect on the sensitivity toward NVP-BKM120 (i.e., IC_{50}) with a *P*-value of 0.38. The average IC_{50} for the *PTEN*-positive cell lines was 1.82 with a SD of 0.98, similar to that for the *PTEN*-negative cell lines (1.60 with a SD of 0.48).

NVP-BKM120 is a PI3K-specific inhibitor and affects only PI3K-mediated signaling

To examine the role of NVP-BKM120 in growth factor-mediated signaling, we tested its effects on serum-starved and EGF-induced glioma cells. Regardless of *p*53 status, NVP-BKM120 inhibited PI3K-mediated signaling by inhibiting the phosphorylation of Akt and S6, (Fig. 2A). Treatment of glioma cells with NVP-BKM120 inhibited PI3K-mediated signaling in a dose-dependent manner.

Comparison of the effect of selective PI3K and mammalian target of rapamycin (mTOR) inhibitors on mTOR signaling revealed differential regulation of S6 and 4E-BP1. Whereas selective inhibition of PI3K by NVP-BKM120 resulted in minor dephosphorylation only of the S6 protein. On the other hand, exposure to the dual PI3K and mTOR inhibitor (NVP-BEZ235) resulted in nearly complete dephosphorylation of both S6 and 4E-BP1 (Fig. 2B).

NVP-BKM120 shows activity in glioma cell lines irrespective of *PTEN* status

We have shown that NVP-BKM120 is active in a broad range of glioma cell lines and that this activity persists even in the background of mutations, such as *PTEN*, that activate signaling through PI3K. First, the dose response for NVP-BKM120 in blocking phosphorylation of Akt and in inducing proliferative arrest did not change as a function of *PTEN* status. We treated U87MG (*PTEN* mutant) and LN18 (*PTEN* wt) cells with increasing concentrations of NVP-BKM120 and analyzed proliferation, cell-cycle distribution, and levels of phosphorylated Akt by immunoblot (Supplementary Fig. S1B). The IC_{50} for inhibiting phosphorylation of Akt was between 0.5 to 1 μmol/L consistent with the range of concentration required to inhibit cell proliferation (Supplementary Fig. S1A) and did not differ dramatically between cells wild-type and mutant at *PTEN*.

NVP-BKM120 arrested cells in G_2 to M phase of the cell cycle

We have further explored the effect of NVP-BKM120 on cell-cycle arrest (Fig. 2C). Control cells showed a typical pattern of cell cycle with 5% to 10% of cells in the G_2 to M phase. The G_2 to M fraction at 72 hours increased in comparison with control cells in both p53-wt (U87) and p53-mutant/deleted (U251) cell lines. In addition, an increasing population of polyploid cells was observed in treated U251 cells. It seems that the NVP-BKM120-treated p53-null cells adapted to NVP-BKM120 inhibition and reentered the cell cycle. U87 cell type has a mixed diploid and polyploid cell population. In addition p53-mutant/deleted (U251) lines show multinucleated cell after NVP-BKM120 treatment (Fig. 2D and E). We used logistic regression to assess the effect between the percentage of multi-nucleated cells and the dose of NVP-BKM120. In the model, we included the dose of NVP-BKM120, the cell line indicator, and their interaction as the covariates. Compared with the U87 cell lines, the U251 cell lines were significantly more likely to have multinucleated cell when treated with NVP-BKM120. Compared with the U87 cell lines, the U251 cell lines were significantly more likely to have multinucleated cell when treated with NVP-BKM120.

Mitotic catastrophe cell death in NVP-BKM120–treated cells and downregulation of Aurora B kinase

Interestingly, NVP-BKM120–treated cells show aberrant segregation of chromosomes, microtubule misalignment, multicentrosomes, or multipolar mitoses. Mitotic perturbances are correlated with mitotic entry frequencies. p53-Mutant/deleted exhibited highest number of mitotic aberrations. Clearly, cells with dysfunctional G_2-M checkpoint (U251, LN18, and LN229) enter more frequently into mitosis on NVP-BKM120 treatment. Multiple centrosomes are characteristic feature of U251 cell line. Chromosome misalignments along the spindle and micronucleated cells were typically encountered in U251 (Fig. 3A). Because low mitotic entrance was reported for p53-wt cell lines (U87), only few aberrant mitotic

figures were present. These data confirm that mitotic catastrophe was the primary mediator of cell death induced by NVP-BKM120.

p53 deficiency induces bypass of the G_2-M checkpoint and premature mitosis after NVP-BKM120

We hypothesized that, on treatment with the drug, the majority of cell lines at first arrest in G_2 stage, with a differential percentage of cells that overcome G_2-M transition checkpoint and enter aberrant mitosis, leading to mitotic catastrophe cell death. If p53 is involved in the checkpoint control, p53-deficient cells will show a higher number of cells in M phase after NVP-BKM120 treatment. Expression of phospho-H3 varied from 1% to 3% in control cells of both p53-wt and p53-mutant/deleted cell lines. After treatment, all cell lines responded with an increase of phospho-H3 (Fig. 3B). U87, D54, and U343 showed 2.6%, 2.8, and 3% of cells in mitosis, respectively, after treatment with NVP-BKM120. Surprisingly, premature mitotic entry in p53-mutant/deleted cells after treatment increased drastically to 12.4%, 7.3%, and 7.9% in U251, LN18, and LN229, respectively. Statistically significant differences in the entrance in mitosis were found between p53-mutant/deleted and p53-wt cells ($P < 0.001$). These data suggested that NVP-BKM120 activates G_2-M checkpoint in p53-wt cells, delaying the movement of G_2 cells into mitosis phase. In contrast, NVP-BKM120 treatment of p53-mutant/deleted cells did not activate G_2-M checkpoint after NVP-BKM120 treatment as those cells largely progressed into mitosis. Alternatively, we have shown that NVP-BKM120 activates a mitosis-specific blockage such as spindle checkpoint or chromosome separation. To gain mechanistic insight into how NVP-BKM120 induced mitotic defects, we examined the effects of NVP-BKM120 on a number of mitotic checkpoint regulators, including cyclin B1, cyclin A, Aurora A, Aurora B, and Cdc2, in U87 and U251 cells treated with 2 μmol/L NVP-BKM120 for indicated periods and found that NVP-BKM120 efficiently depleted Aurora B kinase activity in p53-mutant/deleted cells (U251) in a time-dependent manner (Fig. 3C). Notably, the catastrophic mitotic defects observed in U251 cells and lacking Aurora B signal closely resembled the nuclear morphology of cells in which Aurora B kinase activity is inhibited indicating that mitotic catastrophic death is because of deregulation of Aurora B kinase activity.

Mitotic catastrophe cell death is followed by apoptotic DNA fragmentation

According to the cell-cycle profile, a sub-G_0 increase was detected in cell lines on treatment at 72 hours. It is noteworthy that the sub-G_0 population increment followed decrease in G_2-M block. To further study cells in sub-G_0, the earliest apoptotic marker, Annexin V, was studied. The change of the percentage of apoptosis upon NVP-BKM120 treatment was significantly higher for the p53-wt cell lines (14.52%) than the p53-mutant/deleted cell lines (3.98%) with a P value < 0.0001 (Fig. 4A). Our data indicate that, after 72 hours of treatment, the p53-mutant/deleted cell lines were undergoing predominantly mitotic catastrophe, whereas p53-wt cell lines had preponderance toward apoptotic like death. An increase in PARP and caspase-3 cleavage was observed in a time-dependent manner (Fig. 4B).

Rescue of mitotic catastrophe by p53 knockdown after NVP-BKM treatment

To analyze the effects of NVP-BKM120 on mitotic catastrophy induced by p53 loss, p53 was knocked down by lentiviral shp53 in U87 glioma cells. p53 levels were measured using Western blot analysis 96 hours posttransduction. Transduction with p53 shRNA produced a noteworthy decrease in p53 protein expression (Fig. 5A), and treatment with PI3K inhibitor NVP-BKM120 significantly increased mitotic catastrophy generation as measured by increased number of multinucleated cells (Fig. 5B), microtubule misalignment, multiple centrosomes (Fig. 5C), and increased percentage of phospho-histone–positive cells (Fig. 5D). NVP-BKM120 treatment in p53 knockdown cells lead to decrease on p-Aurora B

kinase (Fig. 5A) indicating that mitotic catastrophic death is because of deregulation of Aurora B kinase activity. These results confirm that NVP-BKM120 exert differential forms of cell death on the basis of p53 status of the cells with p53 wild-type cells undergoing apoptotic cell death and p53-mutant/deleted cells having a mitotic catastrophe cell death.

NVP-BKM120 treatment is well tolerated and effective in an intracranial GBM xenograft model

NVP-BKM120's antitumor efficacy was also evaluated in the U87 xenograft intracranial tumor model of glioma. The median survival time of the control mice (i.e., those injected with NMP/PEG300) was 26 days, whereas the median survival time of the mice orally treated with 20 or 40 mg/kg of NVP-BKM120 once a week for a total of 5 weeks was 38 days and 48 days, respectively. The *in vivo* therapeutic efficacy of NVP-BKM120 was assessed by plotting the Kaplan–Meier survival curves of animals, and group data were compared using the log-rank test (Fig. 6A). Mice treated with NVP-BKM120 had no obvious signs of adverse effects with respect to body weight, water intake, and general activity. *Ex vivo* analyses of tumor tissues obtained from necropsied mice at the end of treatment showed marked inhibition of phosphorylated Akt and phosphorylated S6 in the NVP-BKM120–treated animals (Fig. 6B). The antitumor effect was also evidenced by decreased levels of phosphorylated Akt in the tumor tissues, consistent with a blockade of PI3K, as revealed by immunohistochemical analyses of tumor sections (Fig. 6C).

Immunohistochemical analysis further showed a significant reduction in the percentage of cells expressing Ki-67, control tumors displayed hyper cellular areas with high mitotic numbers, whereas NVP-BKM120–treated cells showed decreased proliferation (Fig. 6C). Consistent with the *in vitro* finding of apoptotic cell death in U87 cell lines by NVP-BKM120 treatment, the *in vivo* U87 model also showed increased cleaved PARP and cleaved caspase-3 staining in tumors treated with NVP-BKM120 treatment further strengthening the fact that NVP-BKM treatment leads to apoptotic cell death in cells with wild-type p53 status (Fig. 6C).

Discussion

Because of the high frequency of genetic alterations in the PI3K/Akt signaling cascade in many types of human cancer, there is intense interest to discover inhibitors of this pathway and evaluate them for therapeutic use. A number of potential therapeutics targeting the PI3K signaling cascade has been generated. The research presented in this report describes the use of a selective pan PI3K inhibitor NVP-BKM120 in a set of well-characterized GBM cell lines with specific features that may affect the inhibitor's mechanism of action.

In our study, we have examined the response of a panel of glioma cell lines to PI3K inhibitor, NVP-BKM120. Our data indicate cytotoxic and cytostatic effect of the drug. Although we have observed a range of IC_{50} in all the glioma cell lines analyzed, we could identify differential form of death between p53-mutant/deleted and p53-wt cells followed by NVP-BKM120 treatment. We found that PI3K inhibitor induced G_2-M arrest in both p53-wt and p53-mutant/deleted cell lines analyzed; however, p53-mutant/deleted cell lines displayed a significant mitotic index increase and cellular and nuclear morphology typical for mitotic catastrophe cell death. Mitotic arrested cells displayed chromosomes missegregation, microtubule misalignment, and multiple centrosomes. Furthermore, as a DNA repair process is impaired in p53-deficient cells, more aberrant mitotic figures were reported in U251, U373, and LN18 cell lines after inhibiting PI3K. The mitotic catastrophe cell death was followed by secondary apoptosis. On the contrary, U87, U343, and D54 cells showed a low increase in mitotic entrance, the cells were arrested in G_2 to M phase of the cycle. The cells died mostly through apoptosis. Aurora B kinase is a chromosomal passenger

protein and plays a crucial role in chromosome condensation, alignment, spindle checkpoints, chromosome segregation, and cytokinesis (32). Impaired regulation of Aurora B expression in human cells causes chromosomal abnormality and instability. Both the expression level and the kinase activity of Aurora B have been found to be upregulated in a variety of human cancers (33, 34). Overexpression of Aurora B results in centrosome amplification and multinucleation in human cells, causing unequal distribution of genetic information and creating aneuploidy cells, one of the hallmarks of cancer (35–38). Depletion of Aurora B or overexpression of a kinase-inactive form in cells would also compromise the spindle checkpoint because the activity of Aurora B is required for checkpoint protein recruitment. Our data also showed Aurora B levels were reduced in p53-mutant/deleted glioma cells treated with NVP-BKM120 cells. In line with the fact that decreased Aurora B leads to phenotypically mitotic defects. These observations support the idea that properly maintained Aurora B levels are essential for successful completion of chromosome segregation. Despite the important function of Aurora B kinase in mitotic progression and cancer development, the mechanisms regulating Aurora B expression through the cell cycle remain largely unknown. In this study, we further showed that knockdown of p53 in p53 wild-type cells rescues the wild-type cells from apoptosis to mitotic catastrophic cell death by PI3K inhibition by NVP-BKM120 further strengthening the finding that NVP-BKM120 exert differential form of cell death on the basis of p53 status.

Current PI3K inhibitors under development are grouped by their specificity, ranging from pure PI3K inhibitors to compounds that block both PI3K and mTOR (dual inhibitors) to pure catalytic mTOR inhibitors, and to inhibitors that block Akt. However, it remains unclear which type of inhibitor would be more effective clinically, isoform-specific inhibitors, pan-PI3K inhibitors or dual inhibitors. Numerous PI3K-targeted compounds, many of which are dual PI3K and mTOR inhibitors, are being introduced into clinical trials. Dual inhibitors like NVP-BEZ235 (39) and XL765 (40) are currently undergoing phase I clinical investigation for treatment of solid tumors. Preclinical data show that NVP-BEZ235 has strong anti-proliferative activity against tumor xenografts that have abnormal PI3K signaling, including loss of *PTEN* function or gain-of-function PI3K mutations (41). Subsequently PI-103, a p110α-specific inhibitor was shown to potently block PI3K signaling in glioma cells through its ability to inhibit both p110α and mTOR (42). Numerous compounds that preferentially target selected isoforms of class I PI3Ks are also under development. For example, PX-866 targets p110α, p110γ, and p110δ, with IC_{50} values in the low nanomolar range (43). GDC0941 is a class I PI3K small molecule inhibitor that is active in many tumor types irrespective of Ras mutational status (44). The XL147 agent is a selective PI3K inhibitor and has shown preclinical efficacy in *PI3K*-, *PTEN*-, and *KRAS*-mutant xenografts (45). In this study we have discussed the effects of NVP-BKM120 —a selective pan class I PI3K inhibitor without mTOR inhibition capacity.

Overall, our present findings establish that NVP-BKM120 inhibits the PI3K signaling pathways, leading to different forms of cell death on the basis of p53 statuses. Our data support a mechanistic rationale by which inhibition of PI3K signaling can augment p53-mediated apoptosis. NVP-BKM120 induced proliferative arrest *in vitro* and inhibited growth of established human tumor xenografts *in vivo*. Given the importance of the PI3K pathway in the malignant phenotype, further optimization of the clinical use of this new compound in the coming years is warranted and should lead to better patient outcomes. We provide here a strong rationale for undertaking clinical trials of NVP-BKM120 in patients with GBM in the very near future.

Supplementary Material

Refer to Web version on PubMed Central for supplementary material.

Acknowledgments

The authors thank Verlene Henry, Jennifer Edge, and Lindsy Homes for conducting the animal studies and Kathryn Carnes (Department of Scientific Publications, The University of Texas M. D. Anderson Cancer Center) for editing the manuscript.

Grant Support This study was supported by the following grants: RO1 CA123304, P5CA127001 (W.K.A. Yung), Accelerate Brain Cancer Cure (W.K.A. Yung and D. Koul), Cancer Center Support Grant (CA16672), National Cancer Institute (CA56041, and CA127001-02A1 to W.K.A. Yung), and Novartis.

References

1. Liu P, Cheng H, Roberts TM, Zhao JJ. Targeting the phosphoinositide 3-kinase pathway in cancer. Nat Rev Drug Discov. 2009; 8:627–44. [PubMed: 19644473]
2. Li J, Yen C, Liaw D, Podsypanina K, Bose S, Wang SI, et al. *PTEN*, a putative protein tyrosine phosphatase gene mutated in human brain, breast, and prostate cancer. Science. 1997; 275:943–7. [PubMed: 9053999]
3. Steck PA, Pershouse MA, Jasser SA, Yung WK, Lin H, Ligon AH, et al. Identification of a candidate tumour suppressor gene, MMAC1, at chromosome 10q23.3 that is mutated in multiple advanced cancers. Nat Genet. 1997; 15:356–62. [PubMed: 9090379]
4. Maehama T, Dixon JE. The tumor suppressor, *PTEN*/MMAC1, dephosphorylates the lipid second messenger, phosphatidylinositol 3, 4, 5-trisphosphate. J Biol Chem. 1998; 273:13375–8. [PubMed: 9593664]
5. Maehama T, Dixon JE. *PTEN*: a tumor suppressor that functions as a phospholipid phosphatase. Trends Cell Biol. 1999; 9:125–8. [PubMed: 10203785]
6. Stommel JM, Kimmelman AC, Ying H, Nabioullin R, Ponugoti AH, Wiedemeyer R, et al. Coactivation of receptor tyrosine kinases affects the response of tumor cells to targeted therapies. Science. 2007; 318:287–90. [PubMed: 17872411]
7. Bianco R, Shin I, Ritter CA, Yakes FM, Basso A, Rosen N, et al. Loss of *PTEN*/MMAC1/TEP in EGF receptor-expressing tumor cells counteracts the antitumor action of EGFR tyrosine kinase inhibitors. Oncogene. 2003; 22:2812–22. [PubMed: 12743604]
8. Mellinghoff IK, Wang MY, Vivanco I, Haas-Kogan DA, Zhu S, Dia EQ, et al. Molecular determinants of the response of glioblastomas to EGFR kinase inhibitors. N Engl J Med. 2005; 353:2012–24. [PubMed: 16282176]
9. Berns K, Horlings HM, Hennessy BT, Madiredjo M, Hijmans EM, Beelen K, et al. A functional genetic approach identifies the PI3K pathway as a major determinant of trastuzumab resistance in breast cancer. Cancer Cell. 2007; 12:395–402. [PubMed: 17936563]
10. Nagata Y, Lan KH, Zhou X, Tan M, Esteva FJ, Sahin AA, et al. *PTEN* activation contributes to tumor inhibition by trastuzumab, and loss of *PTEN* predicts trastuzumab resistance in patients. Cancer Cell. 2004; 6:117–27. [PubMed: 15324695]
11. Samuels Y, Wang Z, Bardelli A, Silliman N, Ptak J, Szabo S, et al. High frequency of mutations of the PIK3CA gene in human cancers. Science. 2004; 304:554. [PubMed: 15016963]
12. Cancer Genome Atlas Research Network. Comprehensive genomic characterization defines human glioblastoma genes and core pathways. Nature. 2008; 455:1061–68. [PubMed: 18772890]
13. Stambolic V, Suzuki A, de la Pompa JL, Brothers GM, Mirtsos C, Sasaki T, et al. Negative regulation of PKB/Akt-dependent cell survival by the tumor suppressor *PTEN*. Cell. 1998; 95:29–39. [PubMed: 9778245]
14. Stokoe D, Stephens LR, Copeland T, Gaffney PR, Reese CB, Painter GF, et al. Dual role of phosphatidylinositol-3, 4,5-trisphosphate in the activation of protein kinase B. Science. 1997; 277:567–70. [PubMed: 9228007]
15. Kennedy SG, Wagner AJ, Conzen SD. The PI 3-kinase/Akt signaling pathway delivers an anti-apoptotic signal. Genes Dev. 1997; 11:701–13. [PubMed: 9087425]
16. Stephens L, Anderson K, Stokoe D, Erdjument-Bromage H, Painter GF, Holmes AB, et al. Protein kinase B kinases that mediate phosphatidylinositol 3,4,5-trisphosphate-dependent activation of protein kinase B. Science. 1998; 279:710–4. [PubMed: 9445477]

17. Elledge SJ, Winston J, Harper JW. A question of balance: the role of cyclin-kinase inhibitors in development and tumorigenesis Harper. Trends Cell Biol. 1996; 6:388–92. [PubMed: 15157521]
18. Sherr CJ, Roberts JM. Inhibitors of mammalian G1 cyclin-dependent kinases. Genes Dev. 1995; 9:1149–63. [PubMed: 7758941]
19. Shtivelman E, Sussman J, Stokoe D. A role for PI 3-kinase and PKB activity in the G_2/M phase of the cell cycle. Curr Biol. 2002; 12:919–24. [PubMed: 12062056]
20. Hammond-Martel I, Pak H, Yu H, Rouget R, Horwitz AA, Parvin JD, et al. PI 3 kinase related kinases-independent proteolysis of *BRCA1* regulates Rad51 recruitment during genotoxic stress in human cells. PLoS One. 2010; 17:e14027. [PubMed: 21103343]
21. Sato N, Mizumoto K, Nakamura M, Ueno H, Minamishima YA, Farber JL, et al. A possible role for centrosome overduplication in radiation-induced cell death. Oncogene. 2000; 19:5281–90. [PubMed: 11077445]
22. Nomura M, Nomura N, Newcomb EW, Lukyanov Y, Tamasdan C, Zagzag D. Geldanamycin induces mitotic catastrophe and subsequent apoptosis in human glioma cells. J Cell Physiol. 2004; 201:374–84. [PubMed: 15389545]
23. Vogel C, Hager C, Bastians H. Mechanisms of mitotic cell death induced by chemotherapy-mediated G_2 checkpoint abrogation. Cancer Res. 2007; 67:339–45. [PubMed: 17210716]
24. Mansilla S, Priebe W, Portugal J. Mitotic catastrophe results in cell death by caspase-dependent and caspase-independent mechanisms. Cell Cycle. 2006; 5:53–60. [PubMed: 16319532]
25. Castedo M, Perfettini JL, Roumier T, Andreau K, Medema R, Kroemer G, et al. Cell death by mitotic catastrophe: a molecular definition. Oncogene. 2004; 23:2825–37. [PubMed: 15077146]
26. Jin S, Tong T, Fan W, Fan F, Antinore MJ, Zhu X, et al. GADD45-induced cell cycle G2-M arrest associates with altered subcellular distribution of cyclin B1 and is independent of p38 kinase activity. Oncogene. 2002; 21:8696–704. [PubMed: 12483522]
27. Agarwal ML, Agarwal A, Taylor WR, Stark GR. P53 controls both the G2/M and the G1 cell cycle checkpoints and mediates reversible growth arrest in human fibroblasts. Proc Natl Acad Sci U S A. 1995; 92:8493–7. [PubMed: 7667317]
28. Maira, M.; Menezes, D.; Pecchi, S. Biological characterization of NVP-BKM120, a novel inhibitor of phosphoinosotide 3-kinase in Phase I/II clinical trials [abstract]. Proceedings of the 101st American Association for Cancer Research Congress; 2010 Apr 17–21; Washington DC. Philadelphia (PA): AACR; 2010. Abstract nr 4498
29. Koul D, Jasser SA, Lu Y, Davies MA, Shen R, Shi Y, et al. Motif analysis of the tumor suppressor gene MMAC/*PTEN* identifies tyrosines critical for tumor suppression and lipid phosphatase activity. Oncogene. 2002; 21:2357–64. [PubMed: 11948419]
30. Liu JL, Sheng X, Hortobagyi ZK, Mao Z, Gallick GE, Yung WK, et al. Nuclear *PTEN*-mediated growth suppression is independent of Akt down-regulation. Mol Cell Biol. 2005; 25:6211–24. [PubMed: 15988030]
31. Lal S, Lacroix M, Tofilon P, Fuller GN, Sawaya R, Lang FF, et al. An implantable guide-screw system for brain tumor studies in small animals. J Neurosurg. 2000; 92:326–33. [PubMed: 10659021]
32. Meraldi P, Honda R, Nigg EA. Aurora kinases link chromosome segregation and cell division to cancer susceptibility. Curr Opin Genet Dev. 2004; 14:29–36. [PubMed: 15108802]
33. Bischoff JR, Anderson L, Zhu Y, Mossie K, Ng L, Souza B, et al. A homologue of Drosophila Aurora kinase is oncogenic and amplified in human colorectal cancers. EMBO J. 1998; 17:3052–65. [PubMed: 9606188]
34. Katayama H, Ota T, Jisaki F, Ueda Y, Tanaka T, Odashima S, et al. Mitotic kinase expression and colorectal cancer progression. J Natl Cancer Inst. 1999; 91:1160–2. [PubMed: 10393726]
35. Araki K, Nozaki K, Ueba T, Tatsuka M, Hashimoto N. High expression of Aurora-B/Aurora and Ipll-like midbody-associated protein (AIM-1) in astrocytomas. J Neurooncol. 2004; 67:53–64. [PubMed: 15072448]
36. Hontz AE, Li SA, Lingle WL, Negron V, Bruzek A, Salisbury JL, et al. Aurora A and B overexpression and centrosome amplification in early estrogen-induced tumor foci in the Syrian hamster kidney: implications for chromosomal instability, aneuploidy, and neoplasia. Cancer Res. 2007; 67:2957–63. [PubMed: 17409401]

37. Ota TS, Suto H, Katayama ZB, Han F, Suzuki M, Maeda M, et al. Increased mitotic phosphorylation of histone H3 attributable to AIM-1/Aurora-B overexpression contributes to chromosome number instability. Cancer Res. 2002; 62:5168–77. [PubMed: 12234980]
38. Tatsuka M, Katayama H, Ota T, Tanaka T, Odashima S, Suzuki F, et al. Multinuclearity and increased ploidy caused by overexpression of the Aurora- and Ipl1-like midbody-associated protein mitotic kinase in human cancer cells. Cancer Res. 1998; 58:4811–6. [PubMed: 9809983]
39. Maira SM, Stauffer F, Brueggen J, Furet P, Schnell C, Fritsch C, et al. Identification and characterization of NVP-BEZ235, a new orally available dual phosphatidylinositol 3-kinase/mammalian target of rapamycin inhibitor with potent *in vivo* antitumor activity. Mol Cancer Ther. 2008; 7:1851–63. [PubMed: 18606717]
40. Cohen RB, Janne PA, Engelman JA, Matrinez P, Nishida Y, Gendreau S, et al. A phase 1 safety and pharmacokinetic (PK) study of PI3K/TORC1/TORC2 inhibitor, XL765 (SAR245409), in combination with erlotinib in patients (pts) with advanced solid tumors. J Clin Oncol. 2010; 28:15s. suppl; abstr 3015.
41. Serra V, Markman B, Scaltriti M, Eichhorn PJ, Valero V, Guzman M, et al. NVP-BEZ235, a dual PI3K/mTOR inhibitor, prevents PI3K signaling and inhibits the growth of cancer cells with activating PI3K mutations. Cancer Res. 2008; 68:8022–30. [PubMed: 18829560]
42. Fan QW, Knight ZA, Goldenberg DD, Yu W, Mostov KE, Stokoe D, et al. A dual PI3 kinase/mTOR inhibitor reveals emergent efficacy in glioma. Cancer Cell. 2006; 9:341–9. [PubMed: 16697955]
43. Koul D, Shen R, Kim YW, Kondo Y, Lu Y, Bankson J, et al. Cellular and *in vivo* activity of a novel PI3K inhibitor PX-866 for treatment of human glioblastoma. Neuro Oncol. 2010; 12:559–69. [PubMed: 20156803]
44. Junttila TT, Akita RW, Parsons K, Fields C, Lewis Phillips GD, Friedman LS, et al. Ligand-independent HER2/HER3/PI3K complex is disrupted by trastuzumab and is effectively inhibited by the PI3K inhibitor GDC-0941. Cancer Cell. 2009; 5:429–40. [PubMed: 19411071]
45. Shapiro G, Kwak E, Baselga J, Rodon J, Scheffold C, Laird AD, et al. Phase I dose-escalation study of XL147, a PI3K inhibitor administered orally to patients with solid tumors. J Clin Oncol. 2009; 27:15s. suppl; abstr 3500.

Translational Relevance

Several components of the phosphatidylinositol-3 kinase (PI3K) pathway are dysregulated in a wide spectrum of human cancers. Gain- or loss-of-function mutants of several components of the pathway lead to neoplastic transformation and therapeutic strategies that target the PI3K pathway are now in development. Small-molecule therapeutics that block PI3K signaling might deal a severe blow to cancer cells by blocking many aspects of the tumor cell phenotype. These facts put the issue of developing targeted drugs for the treatment of cancers that have PI3K pathway dysregulation at the forefront of the translational cancer-research field and one approach is to develop kinase inhibitors for PI3K. NVP-BKM120, a selective pan class I PI3K inhibitor, showed single-agent efficacy in glioma model. Tumor regression was observed in animal models. Preclinical data suggest use of NVP-BKM120 in the treatment of cancers with elevated PI3K signaling. We should soon be in a position to evaluate the clinical success of drugs that are targeted against the PI3K pathway.

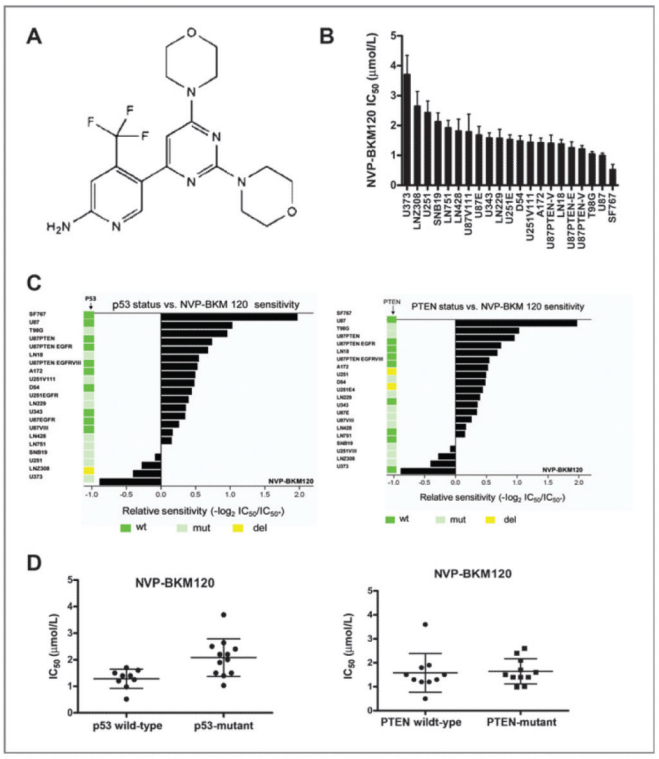

Figure 1.

NVP-BKM120 inhibits glioma cell proliferation. A, structure of NVP-BKM120. B, waterfall plot of IC50 micromolar values. These graphs show that NVP-BKM120 has a particular growth inhibition signature, with some cell lines being exquisitely sensitive and others being relatively resistant. For this, glioma cell lines were plated in 96-well plates at a density of 5,000 cells per well. Cells were treated with increasing concentrations of NVP-BKM120 in triplicate wells for 72 hours, and cell viability was assessed by CellTiter-Blue assay as described in Materials and Methods. The results shown are of a single experiment with 3 independent replicates. C, the relative sensitivity of GBM cell lines to the PI3K inhibitor NVP-BKM120 versus p53 and *PTEN* status. The sensitivity of NVP-BKM120 against the GBM cell lines measured using CellTiter-Blue assay. Indicated values represent the concentration causing 50% growth inhibition (IC_{50}). Values are expressed relative to the mean of IC_{50} of LN751 cell line using the equation: $-\log_2$ (IC_{50} individual cell line/IC_{50} of LN751). D, dot blot showing correlation between p53 and *PTEN* status and *in vitro* drug sensitivity as shown by the IC_{50} of individual cell line. Lines indicate median value. The wild-type p53 cells are more sensitive to NVP-BKM120 than p53-mutant/deleted glioma cells ($P < 0.0001$).

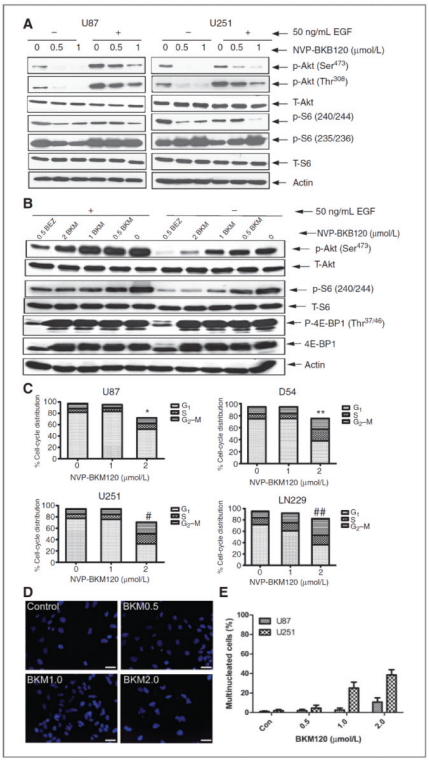

Figure 2.

Molecular responses of human glioma cells to NVP-BKM120. A and B, cell lysates were separated by gel electrophoresis and immunoblotted for phospho-Akt (Ser^{473}), phospho-Akt (Thr^{308}), phospho-S6 ($Ser^{240/244}$ and $Ser^{235/236}$), and phospho-4E-BP1 ($Thr^{37/46}$). Total Akt, total S6, total 4E-BP1, and actin were used as loading controls. C, representative cell-cycle profiles of glioma cells following 72 hours exposure to IC_{50} concentration of NVP-BKM120 represented as stacked columns (*, $P < 0.04$; **, $P < .0001$; #, $P < 0.0001$; ##, $P < 0.0001$). D, accumulation of multinucleated cells in U251 cells exposed to increasing concentrations of NVP-BKM120. Scale bars, 25 μm. E, quantification of multinucleated cells after NVP-BKM120 in glioma cells. Con, control.

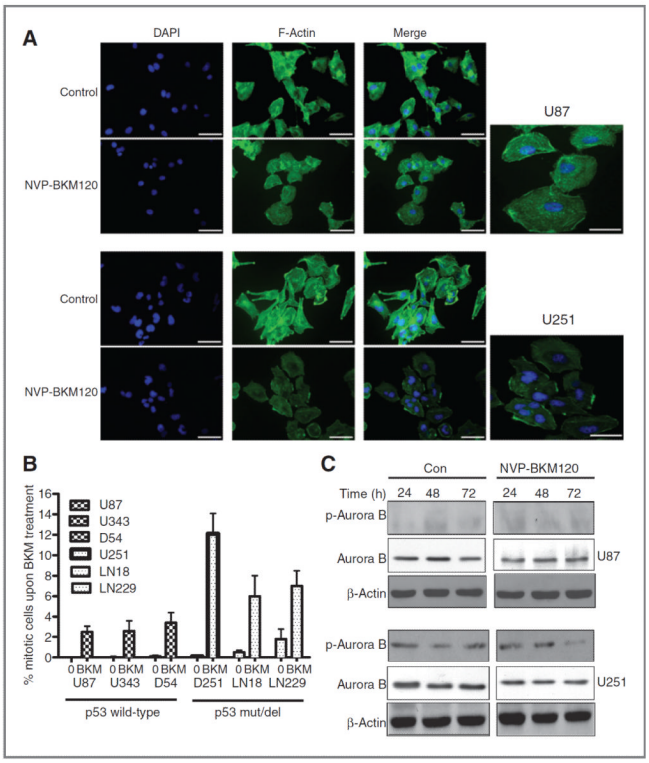

Figure 3.

Mitotic catastrophe cell death on NVP-BKM120 treatment. Seventy-two hours after treatment with 2 μmol/L of NVP-BKM120, cells were collected and immunoassayed with anti-α-F-actin antibody counterstained with 4′,6-diaminidino-2-phenylindole. A, mitotic catastrophe figures showing multiple centrosomes, predominant in U251 cell line. Scale bars, 50 μm. B, significant increase in mitotic entry on treatment with NVP-BKM120 in p53-mutated cell lines. Mean ± SD of 3 independent experiments. Mitotic index in control untreated cells and cells after 72 hours of incubation with PI3K inhibitor is represented. C, Western blot showing p-Aurora B decrease in U251 cells after NVP-BKM120 treatment in a time-dependent manner. β-Actin is used as a loading control. Con, control.

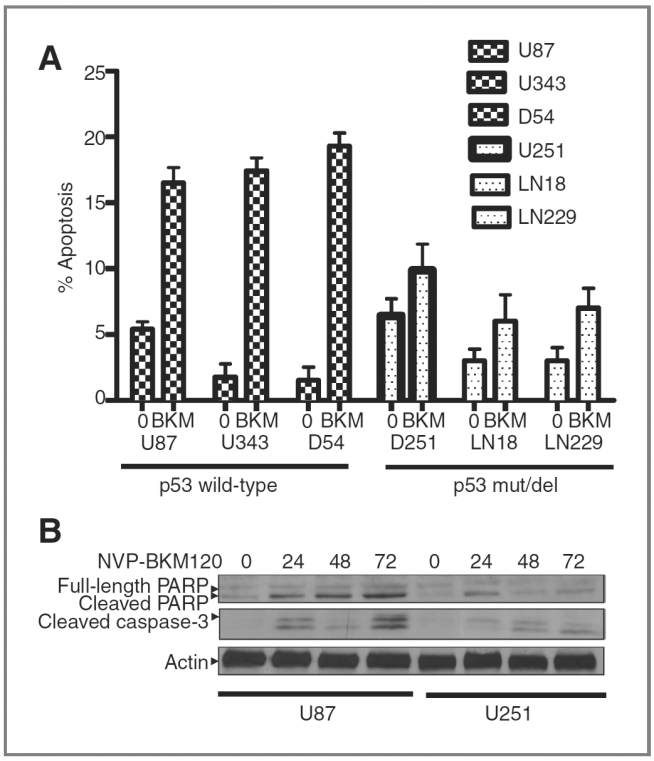

Figure 4.

NVP-BKM120 treatment induces apoptosis in glioma cells containing mutant p53. A, glioma cell lines were treated with 1 and 2 μmol/L NVP-BKM120 for 72 hours before they were harvested for Annexin V staining as an indication of apoptosis. The population of cells positive for Annexin V staining was compiled as shown. U251, LN18, and LN229 cell lines had minimum apoptosis, whereas U87, D54, and U343 cell lines produced maximum Annexin V-positive staining. B, glioma cells were treated with 2 μmol/L NVP-BKM120 for various time intervals, as indicated. Total protein was extracted and subjected for the detection of PARP cleavage and cleaved caspase-3 in a Western blot analysis using an anti-PARP and anti-caspase-3 antibody. Results showed that PARP and caspase-3 were cleaved after NVP-BKM120 treatment in U87 but not in U251 cells.

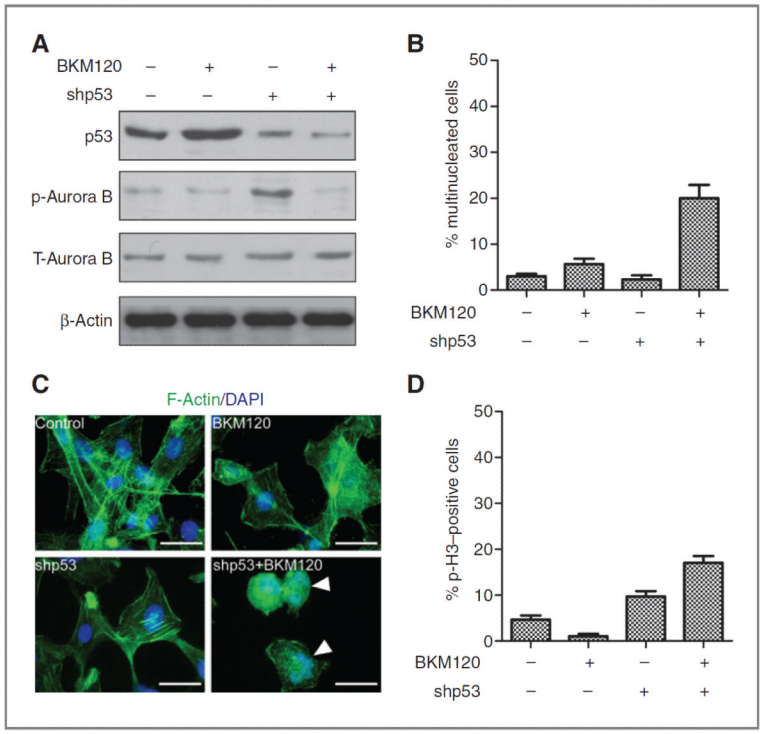

Figure 5.

p53 knockdown restores mitotic catastrophe in U87 glioma cells. A, cell lysates were separated by gel electrophoresis and immunoblotted for p53, p-Aurora B, and Aurora B, and actin was used as loading control. B, quantification of multinucleated cells after NVP-BKM120 in glioma cells. C, p53 knockdown U87 cells were treated with 2 μm of NVP-BKM120; cells were collected and immunoassayed with anti-α-F-actin antibody counterstained with 4′,6-diaminidino-2-phenylindole. Scale bars, 50 μm. D, significant increase in mitotic entry as determined by p-H3-positive cells on treatment with NVP-BKM120 in p53 knockdown U87 cell line. Mean ± SD of 3 independent experiments. Mitotic index in control untreated cells and cells after 72 hours of incubation with PI3K inhibitor is represented.

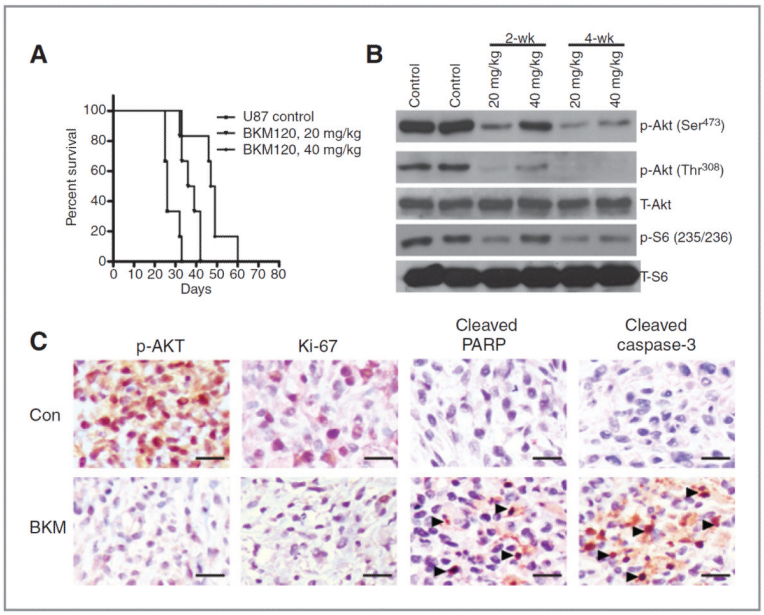

Figure 6.

NVP-BKM120 extends survival in an intracranial animal model. A, U87 cells were implanted intracranially in nude mice ($n = 10$ in each group), and treatment was commenced 4 days later. NVP-BKM120 (20 and 40 mg/kg/d) was administered orally 5 times a week for a total of 20 treatments. The control group mice were treated with NMP/PEG300. Mice were sacrificed at morbidity, and survival curves were compared by using Prism 5 software. The treatment of NVP-BKM120 showed a statistically significant improvement over control ($P = 0.001$ for 20 mg/kg $P = 0.0006$ for 40 mg/kg), as determined by pair-wise log-rank Mantel–Cox test of the Kaplan–Meier survival curves. B, immunoblotting analyses of both the expression and activation of Akt and S6 in 2-week and 4-week tumors following NVP-BKM120 treatment. Immunoblotting analyses showed that NVP-BKM120 inhibited the activity of Akt and S6 in both sets of tumors, as assessed by the level of corresponding phosphorylated protein. C, analysis of NVP-BKM120 effects on tumor xenograft proliferation. Nude athymic mice with established U87 xenografts were treated with vehicle control and NVP-BKM120 (40 mg/kg), tumors were harvested, formalin fixed, and stained for Ki-67 as a marker of proliferation. Tumor sections were stained with antibodies PI3K downstream target p-Akt, apoptotic markers cleaved PARP, and cleaved caspase-3 as described in Materials and Methods. Representative microscopic fields of each immunohistochemical reaction with the overall semiquantitative grading scale. Scale bars, 25 μm. Con, control.

Table 1

Biochemical profile of NVP-BKM120 against selected protein kinases and class I PI3Ks

	Enzyme	IC_{50} (mean ± SD), nmol/L
Class I PI3K	P110α	0.035 ± 0.017
	P110 β	0.175 ± 0.067
	P110 γ	0.348 ± 0.013
	P110 δ	0.108 ± 0.048
	P110α H1047R	0. 058 ± 0.002
	P110α E545K	0. 099 ± 0.006
	P110α E542K	0. 084 ± 0.001
Protein kinases	Fak	>10
	KDR	>10
	PKA	>10
	PKB	>10
	PDK1	>10
	HER-1	>10
	c-Met	>10
	IGF1	>10
	Eph-B4	>10
	FGFR3	>10
	Ret	>10
	Tek	>10
	B-Raf V599E	9.2
	c-Abl	>10
	c-Src	>10
	Jak-2	>10
	mTOR	4.6 ± 1.86

NOTE: All the IC_{50} values are expressed in μmol/L ± SD.